Probing of electronic structures of La@C_{82} superatoms upon clustering realized using glycine nanocavities

2015 Appl. Phys. Express 8 125503

(http://iopscience.iop.org/1882-0786/8/12/125503)

Applied Physics Express **8**, 125503 (2015)
http://dx.doi.org/**10.7567/APEX.8.125503**

Probing of electronic structures of La@C_{82} superatoms upon clustering realized using glycine nanocavities

Atsushi Taninaka[1], Takahiro Ochiai[1,2], Ken Kanazawa[1], Osamu Takeuchi[1], and Hidemi Shigekawa[1*]

[1]*Faculty of Pure and Applied Sciences, University of Tsukuba, Tsukuba, Ibaraki 305-8573, Japan*
[2]*TAKANO Co., Ltd., Miyada, Nagano 399-4301, Japan*
E-mail: hidemi@ims.tsukuba.ac.jp

Received September 29, 2015; accepted November 4, 2015; published online November 25, 2015

We have succeeded in the first direct probe of the change in the electronic structures of La@C_{82} superatoms upon clustering by scanning tunneling microscopy/spectroscopy (STM/STS). An array of ~1.3-nm-diameter glycine nanocavities self-assembled on a Cu(111) surface was used as a template. Isolated La@C_{82} superatoms were stably observed on terraces without diffusion to step edges, which enabled us to observe the change in the electronic structures associated with single, dimer, and clustered La@C_{82}. A cluster with four La@C_{82} superatoms showed electronic structures similar to those obtained for thin films in previous works.

Owing to the electron transfer from the endohedral metal to the fullerene cage to form an atomic structure, endohedral metallofullerenes are called superatoms and have been attracting considerable attention.[1–3] In contrast to the σ and π orbitals of fullerenes, which are highly degenerate and tightly bound to individual C atoms, superatom molecular orbitals (SAMOs) are rather loosely bound to the screening potential of the hollow molecular cage, producing nearly free electron-like characteristics.[1–4] Furthermore, endohedral metallofullerenes are promising candidates for nanotechnological applications because of their electronic and magnetic flexibilities.[1,5–9] However, the formation of isolated structures of endohedral metallofullerenes has been difficult owing to their high reactivity, reducing the high potential for some functions such as catalysis. In addition, despite the importance of understanding the electronic structures of individual endohedral metallofullerenes, studies have generally been carried out on films, for example, those formed on Si surfaces or adsorbed at the steps of metal surfaces.[7,10–13] On the other hand, glycine is known to form an array of nanocavities of ~1.3 nm diameter on a Cu(111) surface by self-assembly, as shown in Fig. 1.[14] Since the diameter of a fullerene is ~1 nm, the array of nanocavities is expected to be a desirable template for studying the electronic structures of individual endohedral metallofullerenes from the fundamental and practical viewpoints.

Here, we demonstrate the first direct probe of the change in the electronic structures of La@C_{82} superatoms upon clustering by scanning tunneling microscopy/spectroscopy (STM/STS) using glycine nanocavities self-assembled on a Cu(111) surface.

La@C_{82} metallofullerenes were prepared by the DC arc discharge method.[1,7] The produced soot was extracted by ultrasonication with carbon disulfide for 2 h, and the residue of the extraction was further refluxed with pyridine for 3 h. The La@C_{82} metallofullerenes were separated and isolated by two-stage high-performance liquid chromatography (HPLC) using a Buckyprep ($\phi 20 \times 250\,mm^2$; Nacalai Tesque) and a Buckyclutcher ($\phi 21 \times 500\,mm^2$; Regis Chemical). The purity of the La@C_{82} sample was higher than 99.9%.[1,15]

After glycine molecular deposition on a clean Cu(111) surface, the obtained surface was annealed at 350 K for 1 h to form an array of glycine nanocavities,[14] and then La@C_{82} molecules were evaporated from a crucible heated at 700 K for 5 s to the Cu surface with the array of glycine nanocavities, which was kept at room temperature (RT). All STM/STS measurements were carried out at ~5 K.

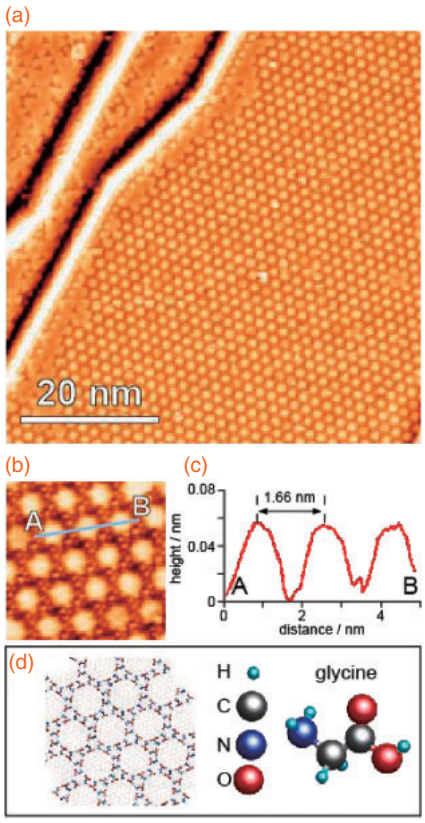

Fig. 1. (a) STM image of Cu(111) surface covered with glycine nanocavities formed by self-assembly ($V_s = -0.15$ V, $I_t = 1.0$ nA). (b) Magnified STM image of the nanocavity array. (c) Cross section along the line in (a). (d) Schematic model of a glycine nanocavity.

Figure 2(a) shows a wide-scan STM image of the La@C_{82}/glycine nanocavities/Cu(111) surface. With the glycine nanocavity template, as expected, La@C_{82} superatoms were stably observed on terraces without diffusion to the step edges, even though the evaporation of La@C_{82} was carried out at RT without cooling. Figure 2(b) shows a magnified image of the area indicated by the square in Fig. 2(a), where the Cu surface in each nanocavity was imaged and formed an array of circles, similar to the image shown in Fig. 1(a). The bare Cu surface is imaged bright because the tunneling current from the area is higher than that above the glycine molecules for this bias

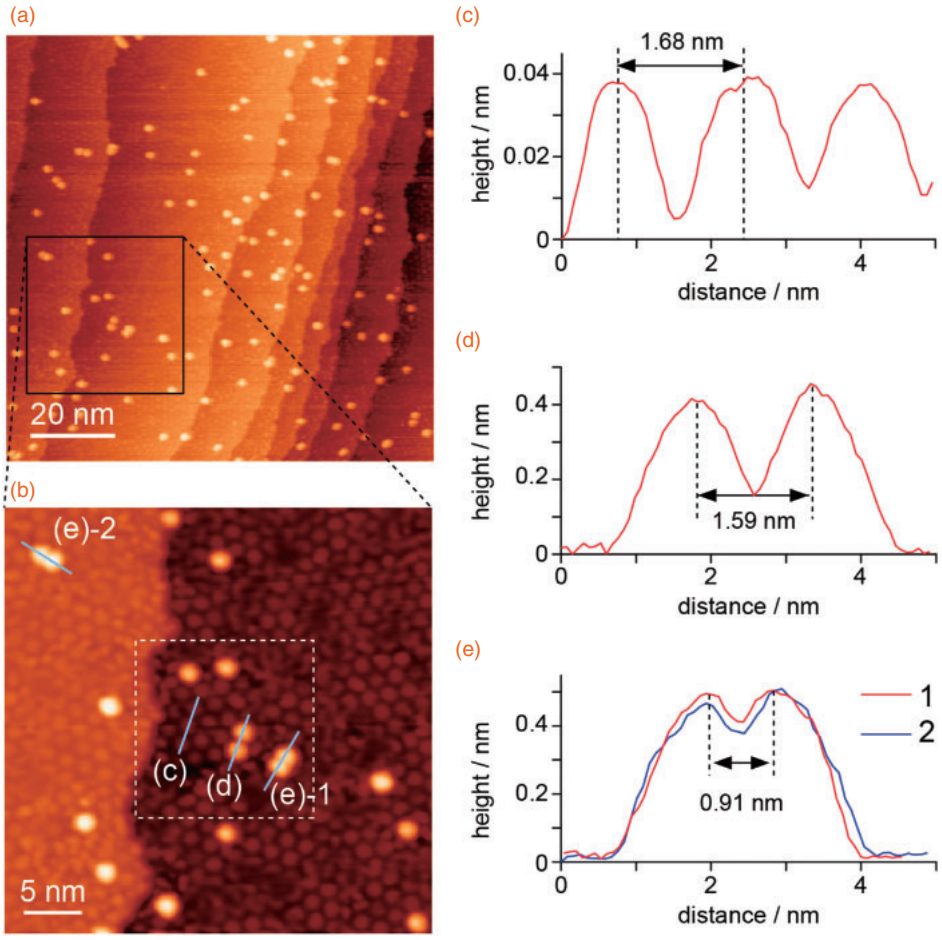

Fig. 2. (a) STM image of the La@C_{82}/glycine nanocavities/Cu surface ($V_s = -0.11$ V, $I_t = 1.0$ nA). (b) Magnified image of the area indicated by the black square in (a) ($V_s = +0.5$ V, $I_t = 1.0$ nA). (c)–(e) Cross sections obtained along the lines shown in (b) labeled (c), (d), (e)-1, and (e)-2, respectively. The lines were drawn from left (low) to right (up).

voltage,[14] and the nanocavity has a structure shown in Fig. 1(d). The circle Cu area is surrounded by six glycine trimers. Since the diameter of each nanocavity is ~1.3 nm (estimated from the circle image in the cavity), La@C_{82} with a diameter of ~1 nm[1,16] ($\lesssim$ 1.3 nm) can be located in the nanocavities. Figures 2(c)–2(e) show the cross sections along the lines (c), (d), (e)-1, and (e)-2 in Fig. 2(b), i.e., a glycine nanocavity, two isolated La@C_{82} superatoms located in neighboring nanocavities, and two La@C_{82} superatoms located close to each other. The distance of 1.59 nm between the two La@C_{82} superatoms shown in Fig. 2(d) is close to the periodicity of 1.68 nm for the nanocavities shown in Fig. 2(c). In contrast, the distance of 0.91 nm between the two La@C_{82} superatoms shown in Fig. 2(e) is close to the diameter of C_{82} (~1 nm), indicating that the structure is a dimer.

Although the heights of the two La@C_{82} superatoms in a dimer are almost the same, the STM images of the two dimers (e)-1 and (e)-2 show a slightly asymmetric shape, depending on the bias voltage, which is more clearly shown for (e)-1 in Fig. 3(a) in the next section. This asymmetry was generally observed in this experiment independent of the ordering of the glycine molecules around La@C_{82}. The effect of the Cu substrate is negligible in the case of La@C_{82} because the additional charge transfer is small.[7,11,17] La@C_{82} has two isomers with different cage structures;[1] however, since the sample was purified by two-stage HPLC in this case, this asymmetry is not due to the mixture of the two isomers. Taking into account the cross sections shown in Figs. 2(c) and 2(e), two bottoms of a dimer may be barely located on a Cu surface in a nanocavity or one of them may be placed above glycine molecules forming corrals. Although the charge transfer is not large, its effect may appear. Another possible mechanism for this is the relative rotation of the two La@C_{82} superatoms in a dimer, as was observed in the case of Ce@C_{82}; that is, Ce@C_{82} with a different adsorption geometry in a film formed on a Cu(111) surface showed different characteristics, especially in terms of the relative intensity in their spectra.[18] For further understanding of this issue, theoretical analysis including the glycine template is necessary.

To observe the electronic structures of the La@C_{82} superatoms, we carried out STS. Figure 3(a) shows a magnification of the area indicated by the white square in Fig. 2(b). The current–voltage (I–V) curves acquired and averaged over the squares on La@C_{82} labeled 1 to 6 are shown in Fig. 3(c). The spectra obtained from the I–V curves in Fig. 3(c) are shown in Fig. 3(e). The four spectra 1 to 4 are similar to each other, showing that the La@C_{82} superatoms with the cross section shown in Fig. 2(d) are isolated and that the interaction between them is small even at a distance of ~0.6 nm (1.59–1 nm). The singly occupied molecular orbital (SOMO) of the La@C_{82} superatom, which is formed by the charge

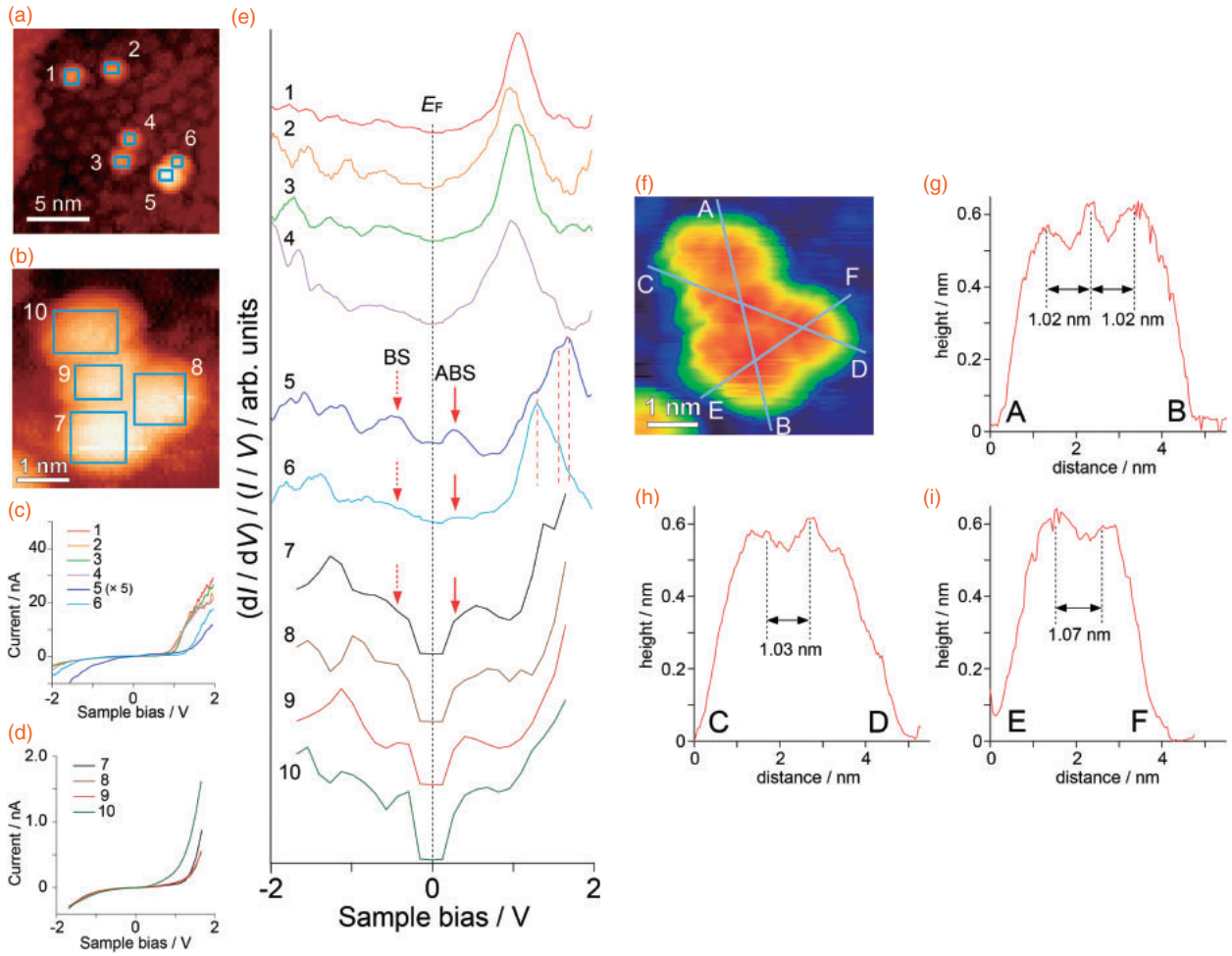

Fig. 3. (a) Magnified image of the area indicated by the white square in Fig. 2(b) ($V_s = -0.8$ V, $I_t = 0.5$ nA). (b) STM image of a La@C_{82} cluster ($V_s = -1.5$ V, $I_t = 1.0$ nA). (c) and (d) *I*–*V* curves obtained over the area indicated by the squares labeled 1–6 in (a) and 7–10 in (b). The intensity of signal 5 is lower than that of 6, which may be due to the fact that the fullerene 5 in the dimer was not in contact with the Cu surface. For the measurements on 7–10, the waiting time to start the *I*–*V* measurement after moving the STM tip to the next grid was shortened to reduce the effects of thermal and mechanical drifts. Therefore, the feedback loop gain was set at a higher value (5%), which resulted in the shift of the set point and a decrease in current intensity. This change does not affect the normalized $(dI/dV)/(I/V)$ spectra. (e) Spectra obtained from the *I*–*V* curves labeled 1–6 in (c) and 7–10 in (d). (f) STM image of the cluster shown in (b) with high contrast. (g)–(i) Cross sections along the three blue lines in (f). Labels A–F correspond to those in (f).

transfer of one electron from La to the lowest unoccupied molecular orbital (LUMO) of fullerene,[1)] is not clear, probably owing to the density of states of the Cu surface near the Fermi level. The signals around 1 V are considered to indicate the density of states related to the hybrid orbitals of unoccupied states of the La@C_{82} superatom, as previously reported.[1,10,15,17,18)] The electronic structures of endohedral metallofullerenes are very complicated. For example, as shown in Fig. 2 in Ref. 11, Fig. 5(b) in Ref. 15, and Fig. 3 in Ref. 18, one STS peak is considered to include some degenerate and quasi-degenerate orbitals that have spatial distributions. Therefore, it is difficult to assign the STS peaks at higher energy regions here.

In contrast, spectra 5 and 6, measured and averaged over the two squares on the dimer labeled 5 and 6, are different from those obtained for the isolated La@C_{82} superatoms. The hybrid orbitals observed at ~1 eV in spectra 1 to 4 clearly shifted toward a higher energy in spectra 5 and 6. The difference in the hybrid orbitals between spectra 5 and 6 is not caused by the shift but by the changes in the intensities of the three peaks indicated by the three red dashed lines. Since hybrid orbitals are complex, the origin of these peaks is not clearly determined at present. The two peaks appeared as indicated by BS and ABS in Fig. 3(e). Taking into account the characteristic of the electronic structures of the superatoms, i.e., the existence of SOMOs, the two peaks BS and ABS are considered to be assigned to the bonding and antibonding states, respectively, which were produced by the bonding of the SOMOs. The SOMO is not degenerated and its position is similar to those observed in previous works.[1,10,15,17)] The difference in intensity between the peaks BS and ABS and that in the hybrid orbitals between spectra 5 and 6 are considered to be caused by the asymmetry of the two La@C_{82} superatoms in a dimer, which was discussed above. To understand the spectra in more detail, theoretical calculations are necessary. However, since La@C_{82} has a SOMO, theoretical analysis with the optimization of the La state is rather difficult at present, which is left for future work.

To examine the observed difference in electronic structure between an isolated La@C_{82} superatom and a dimer structure, we carried out STS measurement on the cluster shown in Fig. 3(f), in which four La@C_{82} superatoms are connected to each other. As shown in Figs. 3(g)–3(i), the distance between the two La@C_{82} superatoms in the cluster was

~1 nm, which is close to that in the dimer shown in Fig. 2(e), indicating that the superatoms are bound to each other. The *I*–*V* curves and the spectra obtained over the blue squares in Fig. 3(b) are shown in Figs. 3(c) and 3(e), respectively. The characteristic structures of the spectra coincide with that previously obtained for a La@C_{82} film formed on a hydrogen-terminated Si(001) surface,[15] as the peaks of BS and ABS were broadened with the formation of the cluster of four La@C_{82} superatoms, suggesting that the electronic structure becomes bulk-like in a cluster of this size.

To understand the observed characteristics in more detail, it will be interesting to analyze the electronic structures of trimers consisting of an odd number of La@C_{82} superatoms in which a single spin remains. Unfortunately, all the trimer-like structures observed in this experiment had a structure in which three La@C_{82} superatoms were located in three neighboring nanocavities. This experiment is under consideration using STM with the equipment for applying a magnetic field to characterize the spin effects. In any case, these experiments can be realized using a glycine nanocavity template. As shown in previous works,[11–13,15,18] the electronic structures of M@C_{82} (M: lanthanoid) have spatial distributions. Here, spatially averaged spectra were considered in the present work because we were interested in the change in nonlocalized SOMO upon clustering. Taking into account the rotation of molecules under STS measurement, a lower set-point current condition used in Ref. 12 should be adopted for the discussions including local electronic structures. A more detailed study with theoretical analysis is expected to open new insights into the physics of superatoms.

In conclusion, we have succeeded in the first direct probe of the electronic structures of La@C_{82} superatoms upon clustering using an array of glycine nanocavities self-assembled on a Cu(111) surface as a template. Isolated La@C_{82} superatoms were stably observed on terraces without diffusion to step edges. In addition to the change in hybrid orbitals of around 1 V, two peaks appeared near the Fermi level after the formation of a dimer structure; such peaks are attributed to the bonding and antibonding states of the SOMO of La@C_{82} superatoms. A cluster with four La@C_{82} superatoms showed electronic structures similar to those obtained for thin films in previous works. Further experiments with theoretical analysis on these results are expected to open new insights into the physics of superatoms.

Acknowledgment H.S. acknowledges the support from the Japan Society for the Promotion of Science (Grant-in-Aid for Scientific Research, 15H05734).

1) H. Shinohara, Rep. Prog. Phys. **63**, 843 (2000).
2) M. Feng, Y. Shi, C. Lin, J. Zhao, F. Liu, S. Yang, and H. Petek, Phys. Rev. B **88**, 075417 (2013).
3) T. Huang, J. Zhao, M. Feng, H. Petek, S. Yang, and L. Dunsch, Phys. Rev. B **81**, 085434 (2010).
4) M. Feng, J. Zhao, and H. Petek, Science **320**, 359 (2008).
5) H. Kato, Y. Kanazawa, M. Okumura, A. Taninaka, T. Yokawa, and H. Shinohara, J. Am. Chem. Soc. **125**, 4391 (2003).
6) J. Zhao, X. Huang, P. Jin, and Z. Chen, Coord. Chem. Rev. **289–290**, 315 (2015).
7) T. Sakurai, X. D. Wang, Q. K. Xue, Y. Hasegawa, T. Hashizume, and H. Shinohara, Prog. Surf. Sci. **51**, 263 (1996).
8) R. M. Brown, Y. Ito, J. H. Warner, A. Ardavan, H. Shinohara, G. A. D. Briggs, and J. J. L. Morton, Phys. Rev. B **82**, 033410 (2010).
9) Y. Ito, J. H. Warner, R. Brown, M. Zaka, R. Pfeiffer, T. Aono, N. Izumi, H. Okimoto, J. J. L. Morton, A. Ardavan, H. Shinohara, H. Kuzmany, H. Peterlik, and G. A. D. Briggs, Phys. Chem. Chem. Phys. **12**, 1618 (2010).
10) C. Ton-That, A. G. Shard, S. Egger, A. Taninaka, H. Shinohara, and M. E. Welland, Surf. Sci. **522**, L15 (2003).
11) M. Grobis, K. H. Khoo, R. Yamachika, X. Lu, K. Nagaoka, S. G. Louie, M. F. Crommie, H. Kato, and H. Shinohara, Phys. Rev. Lett. **94**, 136802 (2005).
12) M. Iwamoto, D. Ogawa, Y. Yasutake, Y. Azuma, H. Umemoto, K. Ohashi, N. Izumi, H. Shinohara, and Y. Majima, J. Phys. Chem. C **114**, 14704 (2010).
13) K. D. Wang, J. Zhao, S. F. Yang, L. Chen, Q. X. Li, B. Wang, S. H. Yang, J. L. Yang, J. G. Hou, and Q. S. Zhu, Phys. Rev. Lett. **91**, 185504 (2003).
14) K. Kanazawa, A. Taninaka, H. Huang, M. Nishimura, S. Yoshida, O. Takeuchi, and H. Shigekawa, Chem. Commun. **47**, 11312 (2011).
15) A. Taninaka, K. Shino, T. Sugai, S. Heike, Y. Terada, T. Hashizume, and H. Shinohara, Nano Lett. **3**, 337 (2003).
16) E. Nishibori, M. Takata, M. Sakata, H. Tanaka, M. Hasegawa, and H. Shinohara, Chem. Phys. Lett. **330**, 497 (2000).
17) C. Ton-That, M. E. Welland, J. A. Larsson, J. C. Greer, A. G. Shard, V. R. Dhanak, A. Taninaka, and H. Shinohara, Phys. Rev. B **71**, 045419 (2005).
18) K. Muthukumar, A. Stróżecka, J. Mysliveček, A. Dybek, T. J. S. Dennis, B. Voigtländer, and J. A. Larsson, J. Phys. Chem. C **117**, 1656 (2013).